SRR-88-01

Testing of an Old Short Span Slab-on-Girder Bridge

Ontario

Ministry of Transportation

Research and Development Branch

89-031512

Technical Report Documentation Page

Testing of an Old Short Span Slab-on-Girder Bridge

Author(s):	B. Bakht, Principal Research Engineer
Number:	SRR-88-01
Date of Publication:	June 1988
Ministry Contact:	Mr Baidar Bakht (416) 235-4674
Abstract:	This report describes the testing and evaluation of an old slab-on-girder bridge with a span of 16.3 m. The bridge, called the Belle River Bridge, comprises a non-composite concrete deck on seven rolled steel girders. This bridge was found to be substandard by analytical evaluation. Proof testing, however, showed that the bridge did not require any posting. The report identifies bearing restraint as the main factor responsible for the extra reserve strength which could not be accounted for by the analytical evaluation.
Comments:	
Key words:	bearing restraint, composite action, evaluation, load distribution, slab-on-girder bridge, testing
Distribution:	Head Office and regions, selected structural engineers
Copyright Status:	Crown copyright © 1988 Ministry of Transportation

SRR-88-01

Testing of an Old Short Span Slab-on-Girder Bridge

B. Bakht
Principal Research Engineer
Structures Research
Research and Development Branch

Published by
The Research and Development Branch
Ontario Ministry of Transportation
Hon. Ed Fulton, Minister
D.G. Hobbs, Deputy Minister

Published without prejudice as to the application of the findings.
Crown copyright reserved; however, this document may be reproduced for non-commercial purposes with attribution to the Ministry.

For additional copies, contact:
The Editor, Technical Publications
Room 320, Central Building
1201 Wilson Avenue
Downsview, Ontario
Canada M3M 1J8

Telephone: (416) 235-3480
CNCP Dialcom Electronic Mail: 23:MIN006

June 1988

Contents

1 Test Summary 1
2 Bridge Description 1
3 Analytical Evaluation 2
4 Details of Instrumentation 2
5 Details of Loading 2
6 Observed Behaviour 3
6.1 Girder Strains at Mid-Span 3
6.2 Girder Deflections at Mid-Span 3
6.3 Girder Strains near an Abutment 3
6.4 Strains in a Diaphragm 4
7 Effects of Bearing Restraint 4
7.1 Analytical Study 4
8 Calculation of Girder Moments from Measured Strains 5
8.1 Procedure 5
8.2 Moments by Ignoring Bearing Restraint Forces 7
8.3 Moments by Including Bearing Restraint Forces 7
9 Reappraisal of Analytical Evaluation 8
10 Discussion of Results 8
10.1 Positions of Neutral Axes 8
10.2 Random Variation of Girder Rigidities 9
10.3 Observations about Bearing Restraint Forces 10
11 Conclusions 10
12 Acknowledgements 11
References 11

1 Test Summary

Bridge:	Belle River Bridge, County of Essex, MTC Site No. 6-94
Type of Bridge:	Slab-on-girder bridge with steel girders and non-composite concrete deck slab.
Date of Construction:	1953
Posted Load:	No posting
Span/width:	16.3/9.1 m
Angle of skew:	0°
Date of test:	July 18, 1985
Test engineers:	Baidar Bakht and Geoffrey Leach
Job Captain:	Zdislaw Knobel
Supervisor instrumentation:	Bill Kwok
Maximum applied load:	One vehicle with a gross weight of 890 kN (91 tonnes), and two side-by-side vehicles, each with an average gross weight of 774 kN (79 tonnes) were brought on the bridge at crawling speed.
Responses measured:	Strains and deflections of all girders and an intermediate diaphragm.

2 Bridge Description

A view of the Belle River bridge is shown in Fig.2.1; it is a slab-on-girder bridge with a 150 mm thick concrete deck slab on seven rolled steel girders. The span and width of the bridge are 16.3 and 9.1 m, respectively. There are two 4.5 m wide traffic lanes and no side walk on the bridge. No mechanical shear connection is provided between the deck slab and girders. The bridge is provided with four diaphragms, one at each support and one at each of the third span points. The cross-section of the bridge is shown in Fig. 2.2 which also shows the sizes of girders and diaphragms. The deck slab carries a 75 mm thick layer of asphalt. Each girder rests on 300 x 300 mm steel bearing plates at each of it ends.

The following observations are made about the condition of the bridge.

a. As shown in Fig.2.3, the girders show some deterioration with corrosion. At one location near an abutment, the bottom flange thickness has been reduced from 19 to about 13 mm.

b. Also as shown in Fig. 2.3, there is evidence of leaking of water through the deck slab.

c. There is a longitudinal crack in the asphalt layer over the second girder from the east in the southern half of the bridge.

d. The drainage pipes are badly corroded, as shown in Fig. 2.4.

e. The mass concrete abutments appear sound except for some minor spalling which is shown in Fig.2.5.

f. Also as shown in Fig.2.5 the bearing plates show signs of moderate corrosion, and some girders appear to be pressing against the ballast wall.

3 Analytical Evaluation

The capacity of the 150 mm thick slab with 0.45% steel to withstand the concentrated loads was found to be 480 kN according to the Ontario Highway Bridge Design (OHBD) Code (1983). Since the minimum required capacity is 392 kN, the deck slab was evaluated to require no posting.

For live load effects due to the OHBD design load, the bridge was analyzed by the grillage analogy method with the mesh shown in Fig. 3.1. The girders were assumed to be non-composite with the deck slab.

The first flexural frequency of the bridge was found to be 4.4 Hz which according to the OHBD code, corresponds to a dynamic load allowance (DLA) of 0.40 for loading in one lane.

The summary of evaluation calculations for a single girder is given in Table 3.1 for two values of the live load factor, namely 1.40 and 1.25. It is recalled that the latter is allowed by the OHBD code when the structure is to be reevaluated within five years. The factored resistances listed in the table do not include a reduction in the moment capacity of a girder caused by the loss of section due to corrosion, which exists mainly near the abutments.

It can be seen in Table 3.1 that even without considering the loss of the girder section due to deterioration, the girder moments due to factored dead and live loads exceed the girder capacity for both the live load factors in nearly all cases, apparently necessitating the posting of the bridge.

It is noted that the maximum girder moments obtained by the grillage method were within about 1% of those obtained by the simplified method specified in the OHBD code.

4 Details of Instrumentation

The response of the structure was monitored through 11 displacement transducers and 45 uniaxial strain measuring devices which consisted of weldable electrical resistance strain gauges and demountable strain transducers. Locations of the instruments and their identifying numbers are shown in Fig. 4.1, and views of the various instruments in Figs. 4.2 through 4.5. Positions of test loads, described in the following section, are shown in Fig. 4.6.

5 Details of Loading

The loads were applied by the two Ministry test vehicles, the axle weights for which are shown in Table 4.1 for the various load levels. Readings of the instruments were taken by positioning either a single vehicle or both vehicles at preselected positions which are shown in Fig. 4.6 along with the identifying numbers. The test vehicles with loads corresponding to load level 0 were first brought onto the bridge. After studying the measured responses, the loads were gradually increased on the vehicles according to the scheme of Table 4.1. For all load levels, the vehicles travelled at crawling speed so as not to induce the dynamic magnification of load effects.

For the load cases involving two side by side vehicles, the loads on the vehicles were raised to level 4 which corresponds to an average gross vehicle weight of 774 kN (79 tonnes). For load cases requiring loading by a single vehicle, the load was raised to level 5 which corresponds to a gross

vehicle weight of 890 kN (91 tonnes). The ratio of maximum gross vehicle weights for loading cases involving two and one vehicles, respectively, is equal to 0.87. It is noted that this ratio compares well with the corresponding modification factor of 0.90 for loading in two lanes as specified by the OHBD code (1983).

6 Observed Behaviour

6.1 Girder Strains at Mid-Span

Longitudinal position No. 4 of the testing vehicles, which is identified in Fig. 4.6, produced the maximum mid-span moments. Accordingly, only the results corresponding to this longitudinal position are presented in this report.

Bottom flange strains in all girders at the mid-span are plotted in Fig. 6.1 for the various transverse positions and load levels of the test loading. It can be seen in this figure that the pattern of transverse distribution of these strains for any load position remains unaffected by the load level, thus confirming the accuracy and repeatability of the instrumentation. Numerical values of the top and bottom flange strains at the mid-span of all the girders are given in Table 6.1 for some vehicle positions with the maximum loading. The strain distributions over the girder depths, as obtained from the measured top and bottom girder strains, are plotted in Fig. 6.2 for various load cases. It is interesting to note in this figure that the position of zero strain, which is often incorrectly regarded as the position of the neutral axis for bending, changes with the load level. As shown in Fig. 6.3, the bottom flange strains vary in nearly a linear fashion with respect to the load levels.

6.2 Girder Deflections at Mid-Span

Measured girder deflections corresponding to the longitudinal load position No. 4, and various transverse load positions and load levels are plotted in Fig. 6.4. It can be seen in this figure that the measured deflections, except for a few cases at lower load levels, have consistent patterns that conform well to the transverse position of loads. Numerical values of girder deflections at the mid-span are listed in Table 6.2 for some load cases at the maximum load levels.

6.3 Girder Strains Near an Abutment

As shown in Figs. 4.1 and 4.4, strain gauges were installed on the bottom flanges of six girders near the north abutment. The purpose of installing these gauges was to measure the effects of bearing restraint on the behaviour of the girders. It was found that the strains developed in the bottom flanges of the girders due to the bearing restraint were indeed substantial. These strains are plotted in Fig. 6.5 for two load levels and several vehicle positions. It can be seen in this figure that the transverse patterns of strains are maintained for different load levels, but that they are not symmetrical under symmetrical loading, thus emphasizing the somewhat random nature of bearing restraint effects.

Numerical values of the bottom flange strains near the north abutment are listed in Table 6.3 for

some load cases corresponding to load levels 4 and 5. The gauge on the third girder from left did not function. Accordingly, no strain values for this girder are given in Table 6.3. However, the values of strains for this girder required for the interpretation of data discussed later in the report, were obtained by graphical interpolation.

6.4 Strains in a Diaphragm

Strains in the instrumented diaphragm were usually smaller than even the accuracy of the strain measuring system. The largest strains were observed when a single vehicle was in longitudinal load position No. 4, and in transverse load position No. 5. As shown in Fig. 4.6, the vehicle is placed most eccentrically in the latter position.

Numerical values of strains in the north intermediate diaphragm are listed in Table 6.4 due to some load cases corresponding to load levels 4 and 5. It can be seen that even under proof loading the maximum strain in the intermediate diaphragm, corresponds to a stress of only about 10 MPa. The small stress in the diaphragm indicates that the diaphragm is not very active in the transverse distribution of loads.

As shown in Fig. 6.6, the measured strains correspond to extremely small bending moments in the diaphragm. The axial forces, however, are somewhat larger in the vicinity of the applied load. Away from the load, the patterns of both axial forces and bending moments appear somewhat irregular. This may be so because the plotted response are calculated from very small strains which in some instances are smaller than the accuracy of the measuring system.

7 Effects of Bearing Restraint

Strains in the bottom flanges of girders near their respective supports are indeed indicative of the bearing restraint forces. However, these forces cannot be accurately computed from the measured strains for the following two reasons.

a. The measured strains comprise not only the strains due to bearing restraint forces, but also the strains due to bending moments at the instrumented section. These latter strains, which were shown by calculations to be significantly large for the case under consideration, cannot be realistically obtained from elementary beam theory, as the assumption of "plane sections remaining plane" does not remain quite valid close to the ends of a beam.

b. Strains due to the bearing restraint force, F, are also expected to be non-linear in the vicinity of the ends of beams. Consequently, the value of F can be calculated only if the shape of the strain diagram over the girder depth is known.

7.1 Analytical Study

To quantitatively assess the two factors discussed above, one girder of the Belle River bridge was analyzed by an elastic, three-dimensional plane-shell finite element program for loads corresponding to a testing vehicle in longitudinal position number 4. As shown in Fig. 7.1, the bottom flange of the girder was restrained against horizontal movement at one end and by a spring of stiffness K

at the other. The girder was analyzed for three different values of K, namely zero, 111 kN/m and infinity. Clearly, the first case corresponds to a girder in pure flexure, i.e., without any bearing restraint, and the last one to one with completely restrained bottom flange.

σ_s is designated as the bottom flange stress near a support as computed directly from measured strain. This stress is indeed the sum of stresses due to the bearing restraint force and due to bending moments. It was found from this analytical study that, as shown in Fig.7.1(a), σ_s stays fairly uniform in the vicinity of the support.

The stresses due to bending moments alone at a section close to an end are shown in Fig. 7.1(c). It can be seen that the actual bottom flange stress is somewhat larger than the corresponding stress obtained from elementary beam theory. From the results of the plane-shell analysis, it was concluded that the actual bending strains at the instrumented section near the support, could be obtained by multiplying the strains calculated by elementary beam theory by a factor of 1.2.

Stresses due to only the bearing restraint force at a section close to the support, are plotted in Fig. 7.1(d). It can be seen that the stress distribution is highly non-linear. From the results of analysis, it was concluded that for the girder under consideration, the magnitude of bearing restraint force F can be approximately determined by multiplying the bottom flange stress with the sum of the area of the bottom flange and 20% of the area of the web.

The flexural stress in the bottom flange at the section under consideration, obtained from elementary beam theory is designated as σ_b; the areas of the bottom flange and web of the girder are denoted as A_f and A_w, respectively. Then, for the girders of the Belle River bridge, the bearing restraint force F is given by:

$$F = (\sigma_s - 1.2\,\sigma_b)\,(A_f + 0.2A_w) \tag{7.1}$$

8 Calculation of Girder Moments from Measured Strains

8.1 Procedure

In the absence of bearing restraint forces, the total moment M, taken by a fully or partially composite girder can be divided into M_L, M_u and Na, where M_L and M_u are moments taken by the naked steel girder and the concrete flange, respectively, bending about their respective axes, and N is the axial force acting in opposite direction in the girder and concrete flange to a lever arm of a.

$$M = M_L + M_u + Na \tag{8.1}$$

As shown by Bakht (1988), the various terms on the right-hand side of the above equation can be obtained as follows.

$$M_L = \sigma_{fb}\, S_b \tag{8.2}$$

$$M_u = M_L(EI_s/EI_g) \tag{8.3}$$

$$Na = \sigma_a\, A\, a \tag{8.4}$$

where σ_{fb} = flexural stress in the bottom flange of the steel girder.
S_b = section modulus of the naked steel girder with respect to the bottom flange.
EI_g = flexural rigidity of the naked steel girder bending about its own neutral axis.
EI_s = flexural rigidity of the concrete slab bending about its own neutral axis.
σ_a = axial stress in the naked steel girder due to axial force N
A = area of cross-section of the naked steel girder
a = lever-arm of the couple due to axial forces N

It is sufficiently accurate to assume that the lever-arm a is equal to the distance between the neutral axes of the concrete flange and the steel girder.

The above equations are valid only if the section is free from external axial forces, such as those induced by the bearing restraint. It follows, therefore, that σ_{fb} and σ_a should be computed from the measured strains after taking away the effects of bearing restraint. This can be done as follows.

Let the stresses computed from measured strains in the top and bottom flanges of the girder at the section under consideration be designated as σ_t' and σ_b', respectively. The bearing restraint force F can be calculated from measured strains by the type of procedure given in Sec. 7.1. The average axial stress σ_{as} due to bearing restraint is obtained by dividing F with the effective cross-sectional area A_c of the composite section.

$$\sigma_{as} = F/A_c \tag{8.5}$$

In the case of a fully composite section, A_c can be calculated readily after a value of the modular ratio is assumed. However, for partially composite bridges such as the one under consideration, it is difficult to assess A_c which for the sake of convenience is assumed to be equal to the area of cross-section of the steel girder alone.

Having thus calculated approximately the value of σ_{as}, values of σ_t and σ_b can be obtained from:

$$\sigma_t = \sigma_t' - \sigma_{as} \tag{8.6}$$

$$\sigma_b = \sigma_b' - \sigma_{as} \tag{8.7}$$

The expressions for obtaining σ_{fb} and σ_a are as follows.

$$\sigma_{fb} = 0.5\,(\sigma_b - \sigma_t) \tag{8.8}$$

$$\sigma_a = 0.5\,(\sigma_b + \sigma_t) \tag{8.9}$$

It is noted that Eqs. (8.8 and (8.9) and Eqs. (8.1) through (8.4) would yield moments at the neutral axis locations. Conceptually, the girders can be regarded as being supported at the neutral axis locations at their ends.

8.2 Moments by Ignoring Bearing Restraint Forces

It is usual, and incorrect, to ignore the effects of bearing restraint forces in the interpretation of test data of slab-on-girder bridges. According to this practice, the stresses obtained by multiplying the measured top and bottom flange strains with the modulus of elasticity of steel, are regarded as σ_t and σ_b, respectively. Thereafter, the moments taken by the various girder and the associated portions of the deck slab can be calculated by using Eqs. (8.1), (8.8) and (8.9). This usual procedure is first followed to see how the sum of thus calculated girder moments compares with the supposedly statically determinate total applied moments at the instrumented section.

Three load cases are randomly selected for this exercise, two of which comprise a single test vehicle each, and one comprises two side-by-side vehicles. The longitudinal positions of axles along the bridge span are shown in Fig. 8.1 for the former two cases together with the corresponding beam moment at the instrumented, i.e., mid-span, section. Moments calculated by the procedure mentioned above for the three load cases are listed in Table 8.1 for each girder and the associated portion of the deck slab. The table also contains the corresponding beam moments and the ratio of the sum of computed girder moments to the beam moments. If the bridge had behaved like a truly simply supported bridge, these ratios would be very nearly equal to 1.0. However, as shown in Table 8.1, these ratios range between 0.64 and 0.69, apparently suggesting that the actual girder moments are from 31 to 36% smaller than the applied moments. The discrepancy between the beam moments and those computed from measured strains by ignoring the bearing restraint effects, can be seen graphically in Fig. 8.2. In this figure the average beam moments are compared with the computed moments for two of the load cases. It can be seen readily that most of the computed girder moments fall below the average beam moments, which clearly is not correct.

The interpretation of the test data in the manner given above, may leave the false impression that the actual moments due to applied load are somehow reduced by up to 36% due to an unexplainable phenomenon. As shown in the following section, the applied load moments are indeed reduced but not by as much as shown by the interpretation of data according to the procedure given above. Further, the cause of this reduction is identified as the forces due to the bearing restraint effect.

8.3 Moments by Including Bearing Restraint Forces

The results of the three load cases dealt with in Sec. 8.2, are now interpreted by taking account of the bearing restraint forces. The assumptions made in this interpretation are as given in Secs. 7.1 and 8.1. The resulting girder moments are given in Table 8.2 along with $\Sigma F\ \bar{y}$ which is the sum of moments at the neutral axis caused by bearing restraint forces in the various girders. The quantity $\Sigma F\ \bar{y}$ is really the measure of applied moment reduction caused by the bearing restraint forces. The net applied moment at a transverse section in a right bridge should be equal to $(M - \Sigma F\ \bar{y})$, where M is the beam moment. It can be seen that the ratio of sum of computed girder moments and the reduced applied moment is now closer to 1.0, ranging from 0.97 to 1.05. It is noted that this departure from 1.0 is likely to have been caused by errors in the calculation of bearing restraint forces from measured strains.

It can be seen in Fig. 8.3 that the girder moments now computed from measured strains are compatible with the average reduced beam moments. It is interesting to note that under symmetrical loading the girders of the apparently symmetrical bridge do not accept loads symmetrically.

Table 8.2 also gives the ratio of $\Sigma F \bar{y}$ and beam moment M. This ratio, which ranges from (-0.15) to (-0.26), is the true indicator of the reduction of applied load moments due to bearing restraint forces. It can be seen that this reduction does not range between 31 and 36% as would have been shown by that interpretation of data which does not take account of the bearing restraint forces.

From results of interpretation of the test data for a large number of cases, it is concluded that the bearing restraint force reduces the live load moments by a minimum of 15%.

9 Reappraisal of Analytical Evaluation

For the bridge under consideration, a single test vehicle at load level 5 is nearly equivalent to the level 3 OHBDC evaluation load multiplied by 1.25 and 1.40, where the former quantity is the live load factor and the latter is equivalent to (1+DLA). Hence the single vehicle at load level 5 can be regarded as the proof load for the bridge when only one lane is loaded. Similarly, following the arguments presented in Sec 5, the two side-by-side test vehicles at load level 4 constitute the proof loading for the two lanes loaded condition.

The girder strains even under the proof test loads were so small as to lead to the conclusion that the structure could have safely withstood even much higher loads. The structure, therefore, can be regarded to be good for not only the factored OHBDC level 3 evaluation loads, but also for much heavier loads.

The conclusion that the structure is not structurally deficient can also be reached by reappraising the analytical evaluation in light of the fact that the bearing restraint reduces live load moments by a minimum of 15%.

When live load moments are reduced by 15%, the maximum factored live and dead load moments due to OHBDC evaluation load levels 1, 2 and 3 corresponding to a live load factor of 1.25, become 1080, 1171 and 1171 kN m, respectively, compared to the factored resistance of 1172 kN m. The fact that the Belle River bridge is not structurally deficient can now also be confirmed even by a conservative analytical evaluation in which the girders are assumed to be acting non-compositely with the deck slab.

10 Discussion of Results

10.1 Positions of Neutral Axes

It is usual to regard the position of zero strain over the girder depth as the position of neutral axis of the girder. As discussed earlier in the report, the moments taken by the girder, and hence the position of flexural neutral axis of a fully or partially composite section can be determined from observed girder strains only after the axial strains due to the bearing restraint force, are discounted. It will be found that after taking account of these axial strains, the location of the neutral axis in a heavily loaded girder is higher than that of zero strain position. This phenomenon can be observed in Fig. 10.1, in which the positions of neutral axes are compared for different load cases, with the

corresponding zero strain positions. It can be concluded that regarding the position of zero strain as the position of the neutral axis, would have resulted in underestimation of the girder capacities.

10.2 Random Variation of Girder Rigidities

As mentioned earlier, the steel girders of the Belle River bridge are not connected with the deck slab through any mechanical shear connection device. Fig. 10.1 shows clearly that in this type of bridge the degree of composite action between the girders and deck slab, which can be quantified by the position of the neutral axis, is quite random. It can be seen that the position of neutral axis for the same girder changes with the transverse position of the load.

The random nature of the neutral axis positions, implies that the effective flexural rigidities of the girders should also be random. The effective moments of inertia, I_e, of the various girders of the bridge were calculated for several load cases from the following expression

$$I_e = M_g / (\sigma_b \bar{y}) \qquad (10.1)$$

where M_g is the moment taken by the girder as computed from observed strains, σ_b is the bottom flange stress after discounting for the stress due to bearing restraint forces (Eq. 8.7), and $\bar{y}$ is the distance of the neutral axis from the bottom flange. The moments of inertia at the mid-span, thus calculated are shown in Fig.10.2 for three randomly picked load cases. It can be seen that the effective moments of inertia of the various girders, and hence their effective flexural rigidities, vary within relatively wide margins. Such random variation of girder flexural rigidities casts a serious doubt on ability to analyze structures such as the one under consideration by deterministic methods. This aspect is discussed further in the following.

There can be temptation to believe that the bounds of load distribution can be obtained by analyzing a bridge like the Belle River bridge by first assuming no composite action between the girders and the deck, and then by assuming the full composite action. Such a belief may not be justifiable, as can be seen in Fig. 10.3 which shows plots of transverse variations of the distribution factors for mid-span girder moments. One plot corresponds to moments computed from test data for a particular load case, and the other two are obtained by the semi-continuum method (Jaeger and Bakht, 1988) for the two bounds of the composite action. Computer program SECAN1 was used for the semi-continuum analysis.

It can be seen in Fig. 10.3 that the pattern of transverse distribution of actual moments is similar in a general way to the two analytical patterns. However, it is also quite random. Unlike the analytical patterns, the actual pattern is far from being symmetrical. In fact, the distribution factor for maximum girder moment is about 10% larger than the corresponding analytical factor for the fully composite bridge. It can be seen that this increase in the factor and departure from symmetry, is probably caused by the middle girder being considerably stiffer than its two adjacent neighbours on the right-hand side. There cannot be any doubt that even the most rigorous deterministic analysis of slab-on-girder bridges without deliberate shear connection between the girders and the deck slab, is at best a close approximation.

10.3 Observations about Bearing Restraint Forces

The total bearing restraint force for one of the single vehicle load cases dealt with in Secs. 8.2 and 8.3, was found to be about 530 kN, and for the other about 630 kN. The total dead and live load reaction on the left hand, i.e. the north, abutment for each of these cases is estimated to be about 800 kN. If the bearing restraint force developed only from friction between the girder and the bearing plate, the average coefficient of friction would have to range between 0.66 and 0.79. Similarly, the average coefficient of friction would have to be about 0.95 for the case with two side-by-side vehicles. Such high values of the coefficient appear likely in light of the highly rusted conditions of both the girders and bearing plates, and the fact that some of the girders appear to be bearing against the ballast wall.

The computed bearing restraint forces F, are plotted in Fig. 10.4 for the same load case for which the mid-span girder moments are plotted in Fig. 10.3. F is regarded as positive when the bearing restraint force pushes the abutment away from the span, and negative when the abutment is pulled towards the span.

It can be seen in Fig. 10.4 that the bearing restraint force at the outer left hand girder location is not only negative, but is also fairly large. The magnitude of this force may first appear contrary to engineering judgement, since the moments in this girder are relatively small as shown in Fig. 10.3. However, this outcome begins to appeal to engineering judgement when the abutment is regarded as a relatively stiff beam supported elastically on one side by the backfill and subjected to bearing restraint forces on the other. As shown in Fig. 10.5, all but one of the bearing restraint forces are pushing this beam towards the backfill. It can be readily appreciated that when the flexural rigidity of the beam is sufficiently large, the beam at the location of the outer left-hand girder will be forced to move towards the backfill thus inducing a negative bearing restraint force in the girder at that location.

As can be seen in Fig. 6.5, bottom flange strains near the north abutment in the outer right-hand girder are always consistently small. This observation suggests that the flexural continuity of the abutment is possibly broken due to a vertical crack in the abutment at the location identified in Fig.10.5.

11 Conclusions

The test on the Belle River bridge has conclusively demonstrated that the reason for slab-on-girder bridges to appear stiffer than believed, is the presence of bearing restraint forces which either develop only due to friction between the girders and their bearings, or may be supplemented by girders bearing against ballast walls. For the structure under consideration the bearing restraint forces helped to reduce the live load moments in the girders by a minimum of 15%. Because of such reduction the structurally suspect Belle River bridge can now be regarded as structurally sound.

It has been demonstrated that the interpretation of test data without accounting for the bearing restraint effects may lead to the conclusion that applied load moments are reduced much more than they actually are.

The effective flexural rigidities of the girders of the Belle River bridge are shown to be so much different from each other, as to make it almost impossible to accurately analyze the structure deterministically for transverse load distribution.

12 Acknowledgements

It is gratefully acknowledged that Secs. 2, 3 and 4 were drawn from a preliminary report by Geoffrey Leach who was the Assistant Project Engineer with the Ministry at the time of the test; he was also responsible for Figs. 6.1 through 6.4 and for conducting the plane-shell finite element analysis of the rolled steel girder, some results of which are reported in Fig. 7.1.

References

[1] Bakht, B., "Observed Behaviour of a New Medium Span Slab-on-Girder Bridge," Structural Research Report SRR-88-02, Ministry of Transportation of Ontario, Downsview, Ontario, 1988.

[2] Bakht, B. and Jaeger, L.G., "Support Restraint in Slab-on-Girder Bridges," paper in preparation.

[3] Jaeger, L.G. and Bakht, B., *Bridge Analysis by Microcomputer*, McGraw Hill Book Co., New York, N.Y., 1988.

[4] *Ontario Highway Bridge Design Code*. Ministry of Transportation of Ontario, Downsview, Ontario, 1983.

Table 3.1/ Comparison of Maximum Load Effects and Resistances for a Non-Composite Girder

Live Load Factor	Response	Factored Dead Load Response	Response Due to Factored Evaluation Load Level			Total Response Due to Factored Dead Load and Evalution Load Level			Factored Resistance
			1	2	3	1	2	3	
1.40	Moment, kN m	435	850	970	970	1285	1405	1405	1172
	Shear, kN	107	307	347	364	414	354	471	1124
1.25	Moment, kN m	435	759	866	866	1194	1212	1212	1172
	Shear, kN	107	274	310	325	381	417	432	1124

Table 4.1/ Axle Weights for the Two Test Vehicles

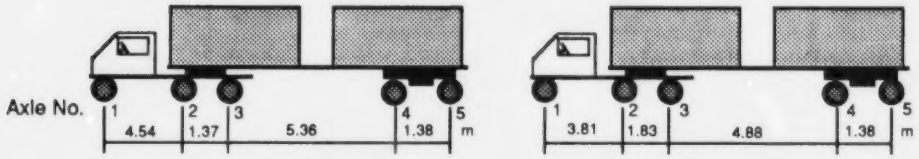

Test Vehicle	Load Level	No. of Concrete Blocks	Weight in kN on Axle No.					Total Vehicle Weight, kN
			1	2	3	4	5	
Kenworth	0	12	45.8	69.8	69.8	73.4	73.4	332
	1	24	47.6	92.5	92.5	105.0	105.0	443
	2	36	49.4	115.2	115.2	136.6	136.6	553
	3	48	51.6	138.3	138.3	168.6	168.6	665
	4	60	53.4	161.5	161.5	200.6	200.6	778
	5	72	55.9	185.2	185.2	231.8	231.8	890
Mack	0	12	42.3	66.7	66.7	71.6	71.6	318
	1	24	43.6	89.9	89.9	104.5	104.5	432
	2	36	44.5	113.0	113.0	137.7	137.7	545
	3	48	45.8	135.7	135.7	169.9	169.9	657
	4	60	46.7	158.8	158.8	202.8	202.8	770
	5	72	47.6	181.0	181.0	236.2	236.2	882

Table 6.1/ Girder at Mid-Span for Longitudinal Load Position No. 4

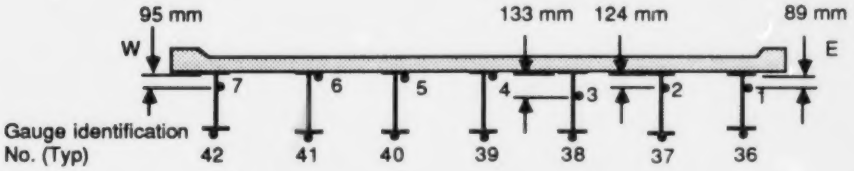

Load Level	Transverse Load Position No.	Gauge Location	Strains mm x 10^6/ mm						
4	4 (2 Trucks)	Top	11	-260	-342	-253	-256	-166	6
		Bottom	82	345	395	443	359	250	118
5	1 (1 Truck)	Top	7	-22	-106	-75	-201	-175	2
		Bottom	10	106	176	274	273	224	100
	2 (1 Truck)	Top	9	-110	-246	-95	-139	-54	6
		Bottom	34	191	251	299	200	125	41
	3 (1 Truck)	Top	8	-230	-290	-64	-48	4	5
		Bottom	77	274	252	217	127	63	11
	5 (1 Truck)	Top	9	0	-63	-51	-199	-226	1
		Bottom	6	81	147	243	283	277	136

NOTE: 1. Compressive strains are shown as -ve
2. For load level see Table 4.1
3. Longitudinal and transverse load positions are identified in Fig.4.6

Table 6.2/ Girder Strains at Mid-Span for Longitudinal Load Position No. 4

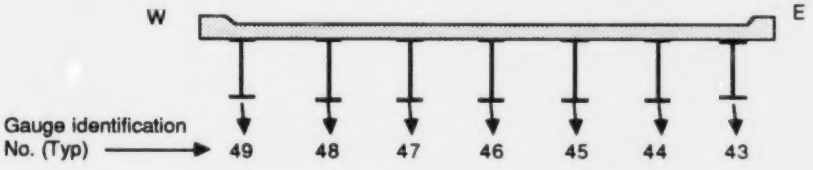

Load Level	Transverse Load Position No.	Downward Deflection in mm at Gauge No.						
		49	48	47	46	45	44	43
4	4	6.6	20.3	28.8	31.3	26.9	18.3	4.7
5	1	0.4	4.1	10.9	16.9	20.2	17.3	4.8
	2	2.3	9.9	18.0	20.4	15.9	8.5	1.6
	3	5.9	16.4	19.7	15.6	8.8	3.4	0.2
	5	0.0	2.5	8.8	14.3	20.3	21.2	6.6

NOTE: 1. Compressive strains are shown as -ve
2. For load level see Table 4.1
3. Longitudinal and transverse load positions are identified in Fig.4.6

Table 6.3/ Bottom Flange Girder Strains Near an Abutment for Longitudinal Load Position No. 4

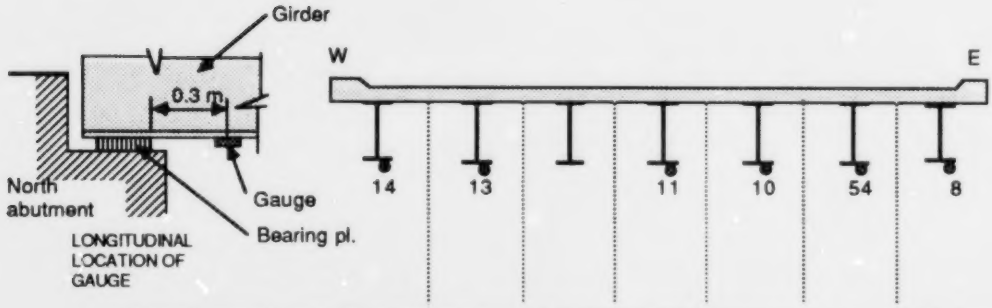

Load Level	Transverse Load Position No.	Strains mm x 10^6/mm at gauge No.						
		14	13		11	10	54	8
4	4	128	-132		-113	-79	4	11
5	1	101	-23		-126	-84	-45	5
	2	115	-80		-125	-8	40	5
	3	67	-127		-56	38	58	6
	5	88	-12		-99	-87	-76	3

NOTE: 1. Compressive strains are shown as -ve
2. For load level see Table 4.1
3. Longitudinal and transverse load positions are identified in Fig.4.6

Table 6.4/ Strains in the North Intermediate Diaphragm for Longitudinal Load Position No. 4

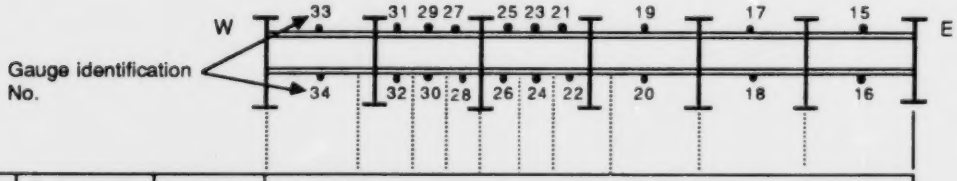

Load Level	Transverse Load Position No.	Gauge Location	Strains mm x 10^6/mm									
4	4	Top	1	0	0	12	5	0	0	5	10	2
		Bottom	7	21	34	-5	4	4	-3	26	20	22
5	1	Top	-1	-3	-3	7	-3	1	-5	0	9	3
		Bottom	-6	-9	-6	-1	0	0	0	17	23	35
	2	Top	0	-5	0	16	2	0	2	6	1	0
		Bottom	-2	3	14	-2	4	22	3	23	8	4
	3	Top	2	0	1	3	7	0	-4	3	0	-1
		Bottom	13	24	36	-5	3	17	1	10	-2	-7
	5	Top	-1	-1	-3	3	-3	-1	4	-2	3	6
		Bottom	-5	-11	-13	0	0	1	-1	10	30	53

NOTE: 1. Compressive strains are shown as -ve
2. For load level see Table 4.1
3. Longitudinal and transverse load positions are identified in Fig. 4.6

Table 8.1/ Girder Moments Computed from Measured Strains by Ignoring Bearing Restraint Effects Due to Vehicle(s) in Longitudinal Position No. 4

Load Level	Transverse Line No.	Computed moment in kN m in girder No.							Σ Computed Girder mt.,kN m ($=M_g$)	Beam mt.,kN m (=M)	$\frac{M_g}{M}$
		1	2	3	4	5	6	7			
4	4	135	383	423	535	358	256	186	2276	3566	0.64
5	2	58	227	301	396	202	144	68	1396	2035	0.69
5	5	14	117	187	334	290	263	212	1417	2035	0.69

Table 8.2/ Girder Moments Computed from Measured Strains by Taking Account of Bearing Restraint Effects

Load Level	Transverse Line No.	Computed moment in kN m in girder No.							Σ Computed Girder mt.,kN m ($=M_g$)	$\Sigma F\bar{y}$	Beam mt.,kN m (=M)	$M-\Sigma F\bar{y}$, kN m ($\bar{M}$)	$\frac{M_g}{\bar{M}}$	$\frac{\Sigma F\bar{y}}{M}$
		1	2	3	4	5	6	7						
4	4	48	535	576	688	469	281	194	2791	-546	3566	3020	0.92	-0.15
5	2	-48	307	401	527	222	118	66	1593	-520	2035	1515	1.05	-0.26
5	5	-63	132	255	433	378	345	116	1596	-387	2035	1648	0.97	-0.19

Note: Vehicles for these load cases were in longitudinal position No.4

Figure 2.1/ View of the Bridge (West Side)

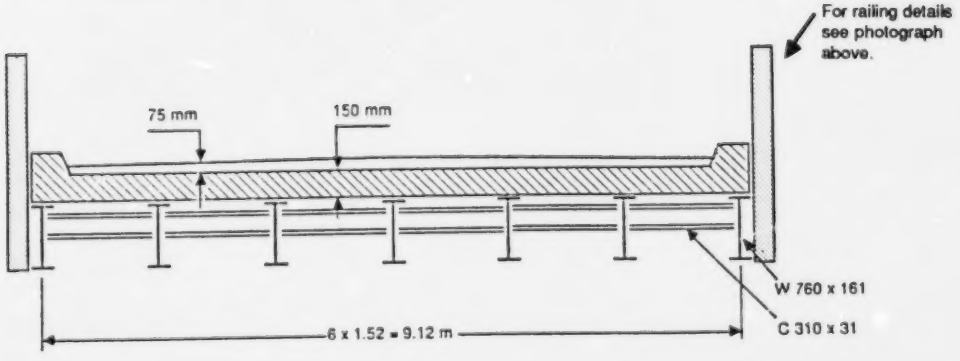

Figure 2.2/ Cross-Section of Belle River Bridge

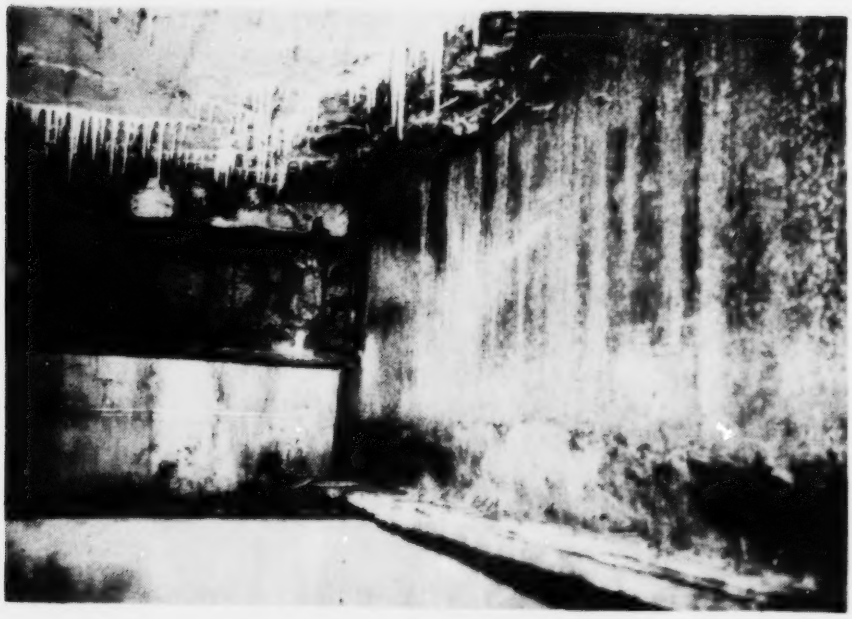

Figure 2.3/ Evidence of Girder Deterioration and Deck Leaching

Figure 2.4/ Corroded Drainage Pipe

Figure 2.5/ Close-up of Bearing Plate

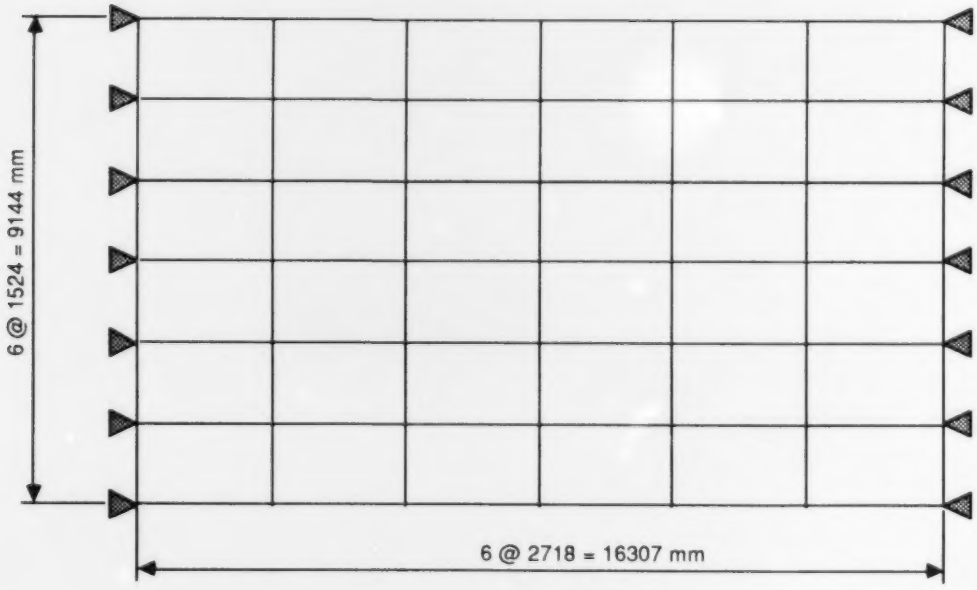

Figure 3.1/ Grillage Mesh Used for Analysis

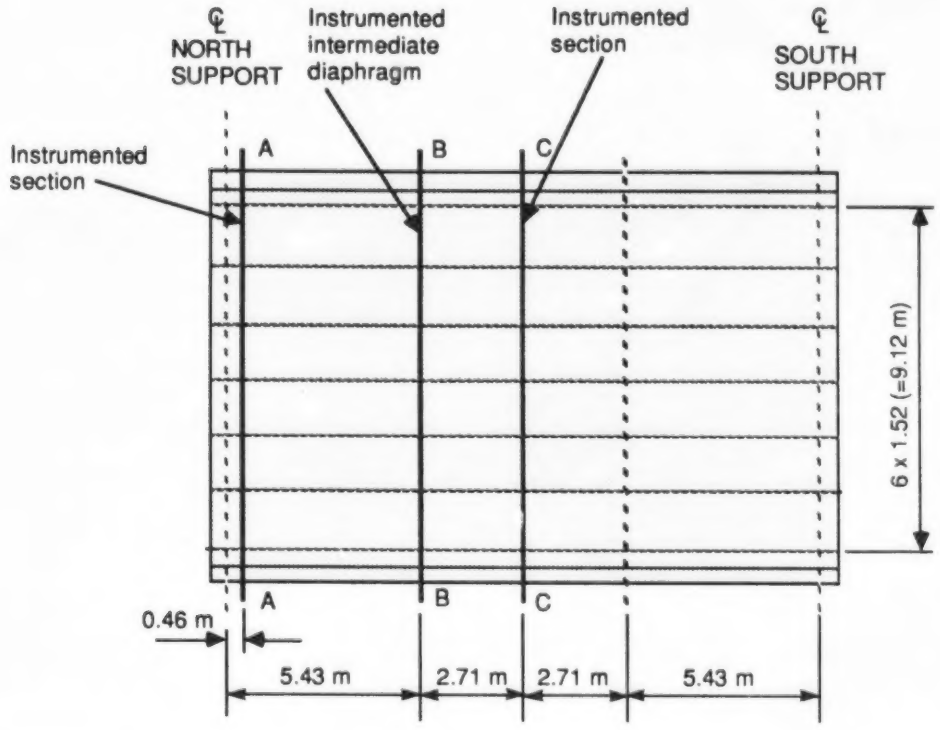

(a) Bridge plan

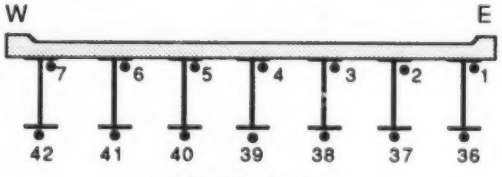

SECTION AT C-C

(b) Strain gauges at mid-span

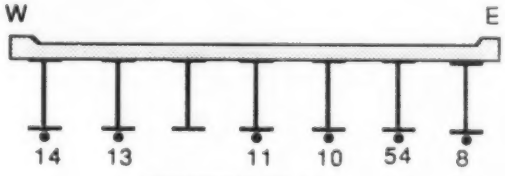

SECTION AT A-A

(c) Strain gauges near north abutment

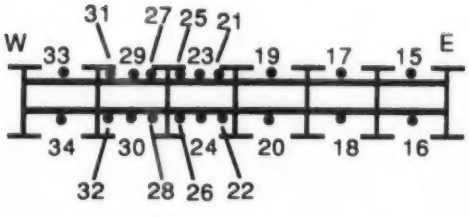

SECTION AT B-B

(d) Strain gauges near on a diaphragm

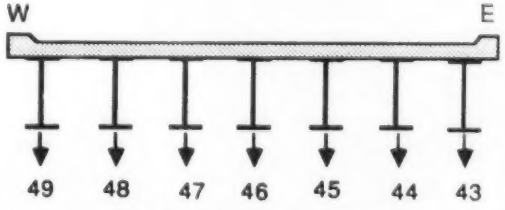

SECTION AT C-C

(e) Deflection transducers at mid-span

Figure 4.1/ Locations of Gauges and their Identifying Numbers

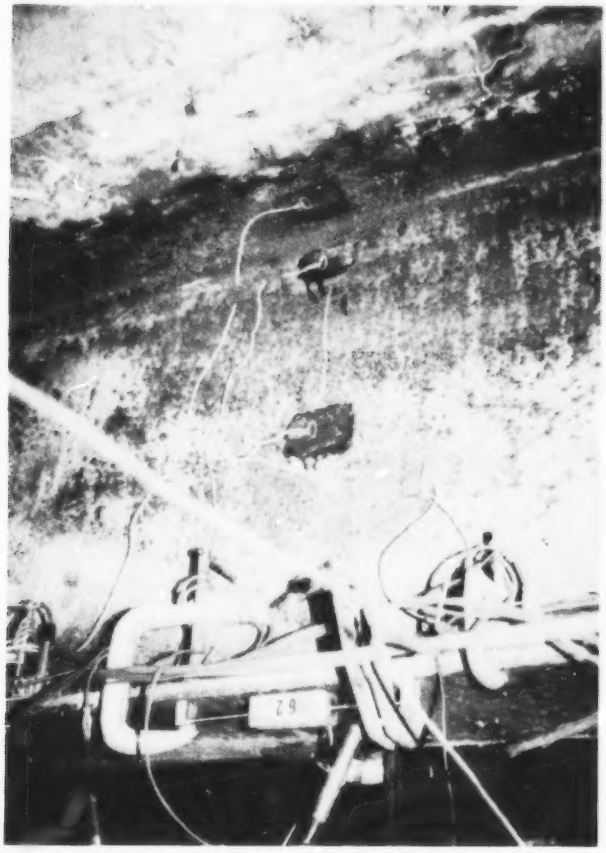

Figure 4.2/ Weldable and Demountable Strain Gauges

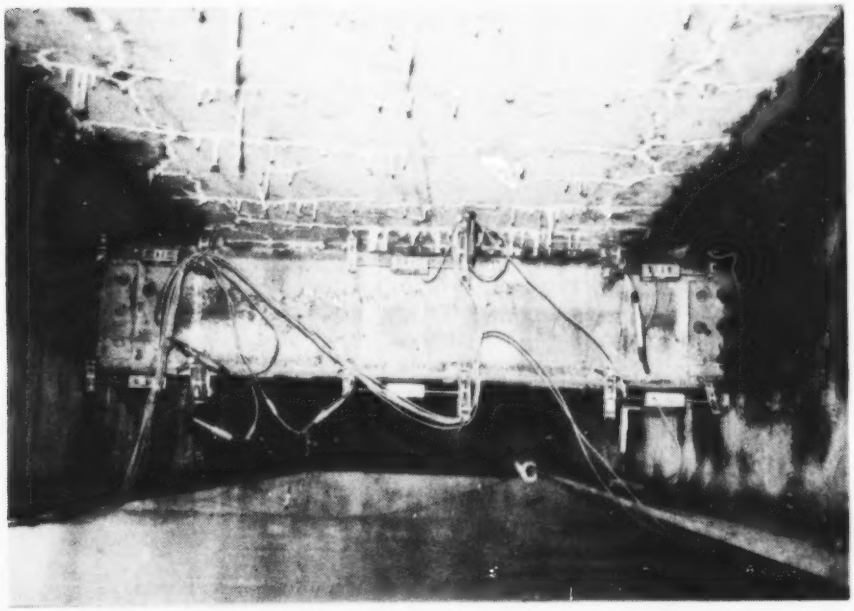

Figure 4.3/ Channel Diaphragm Instrumentation

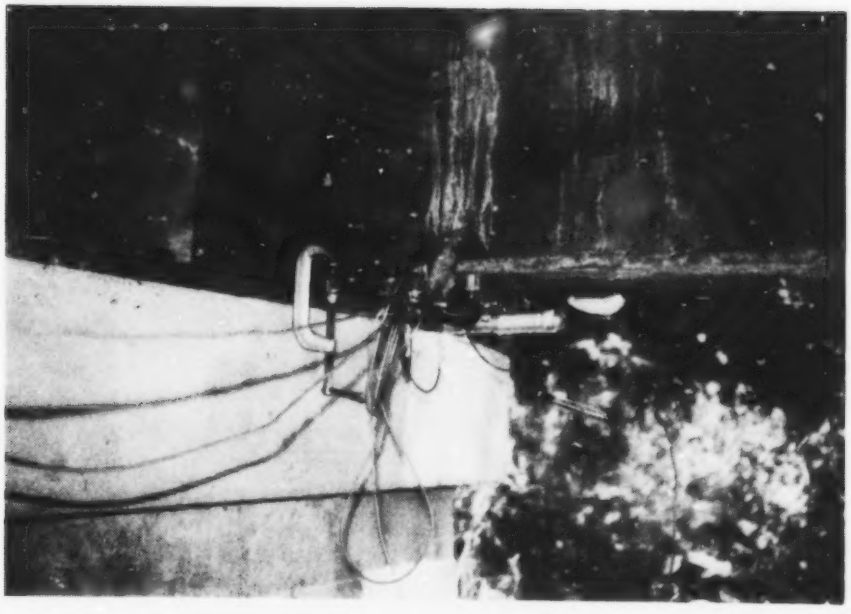

Figure 4.4/ Strain Gauge and Horizontal Transducer at External Girder Bearing

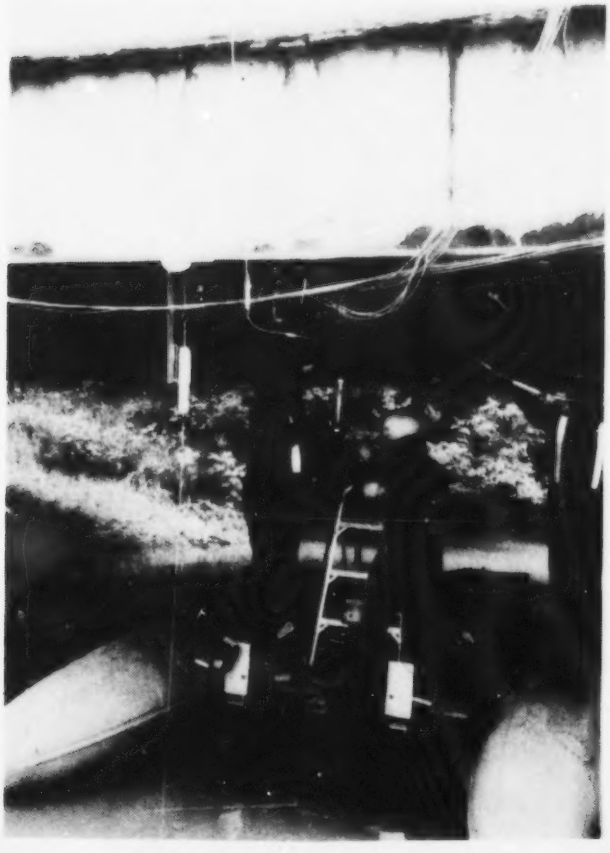

Figuer 4.5/ Vertical Transducers

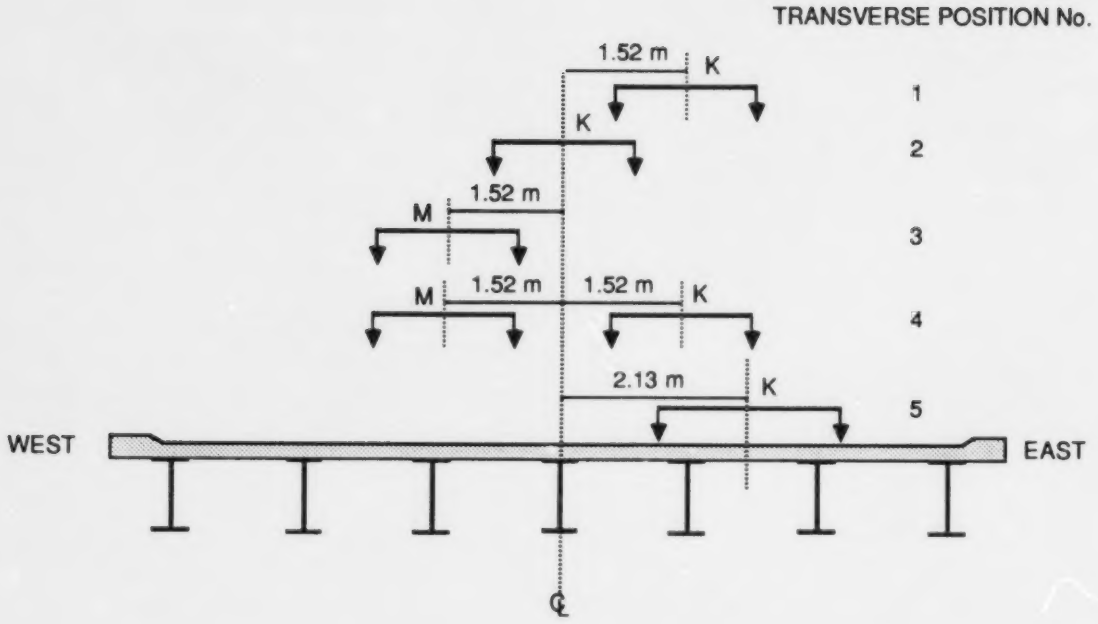

TRANSVERSE VEHICLE POSITION

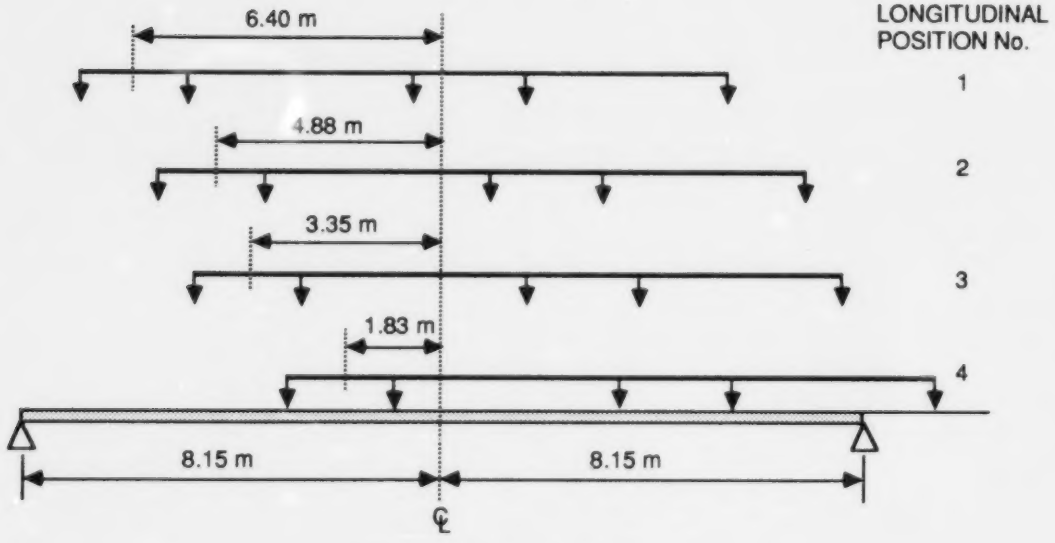

LONGITUDINAL VEHICLE POSITION

NOTE: K and M refer to Kenworth and Mack test vehicles, the axle weights for which are given in Table 4.1

Figure 4.6/ Positions of the Testing Vehicles

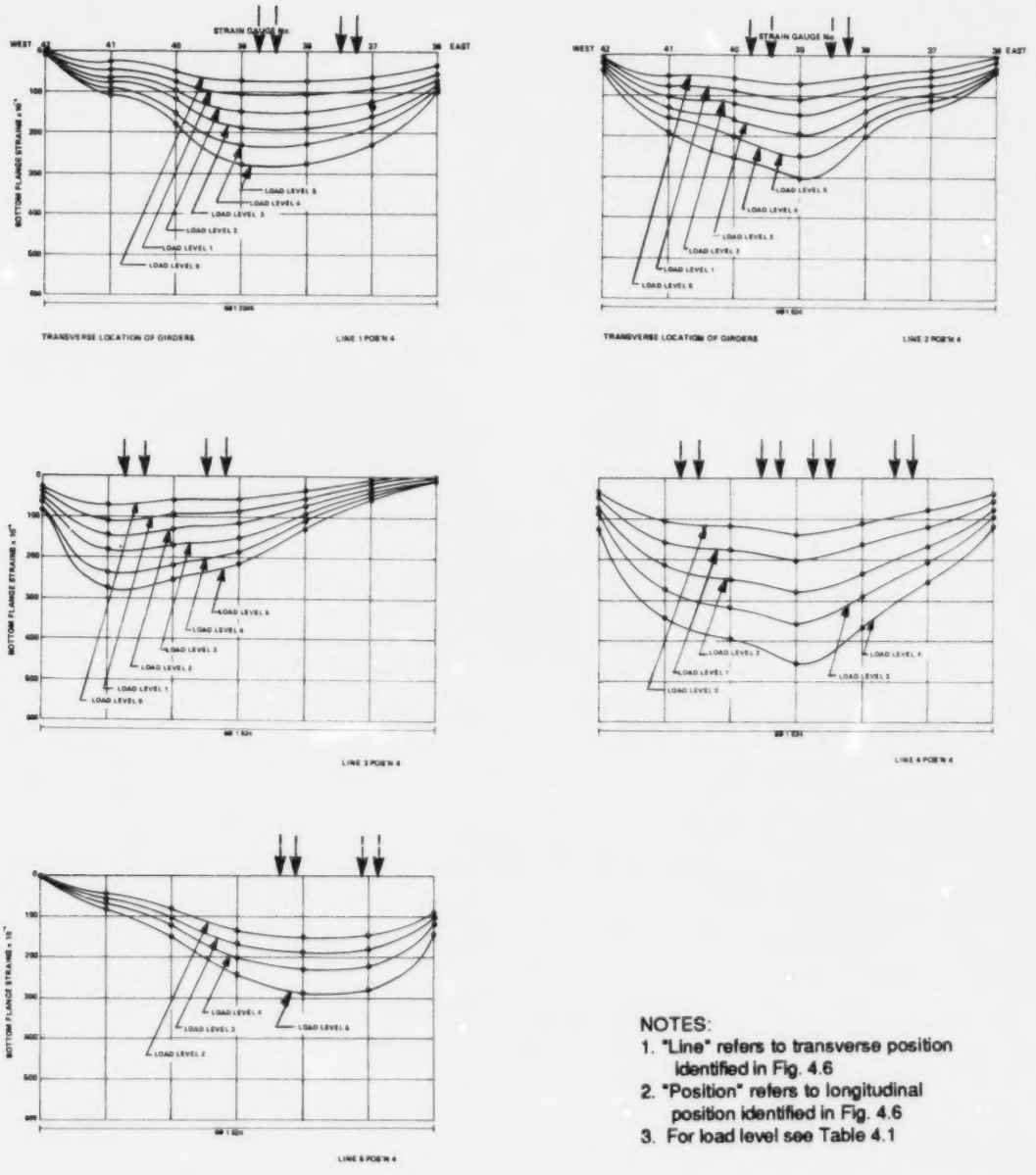

NOTES:
1. "Line" refers to transverse position identified in Fig. 4.6
2. "Position" refers to longitudinal position identified in Fig. 4.6
3. For load level see Table 4.1

Figure 6.1/ Bottom Flange Strains at Mid-Span

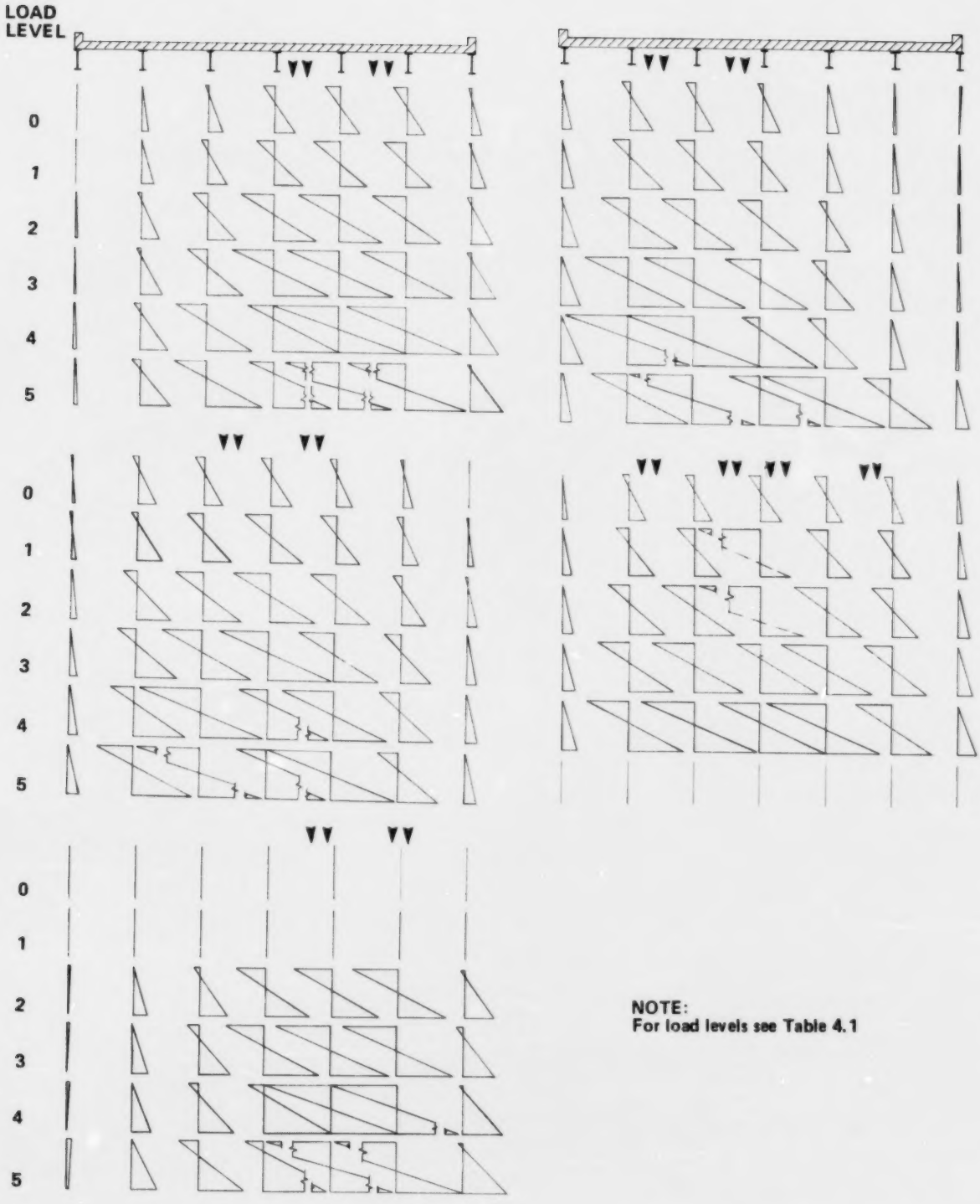

Figure 6.2/ Strain Distribution Over Girder Depth for Longitudinal Position no. 5

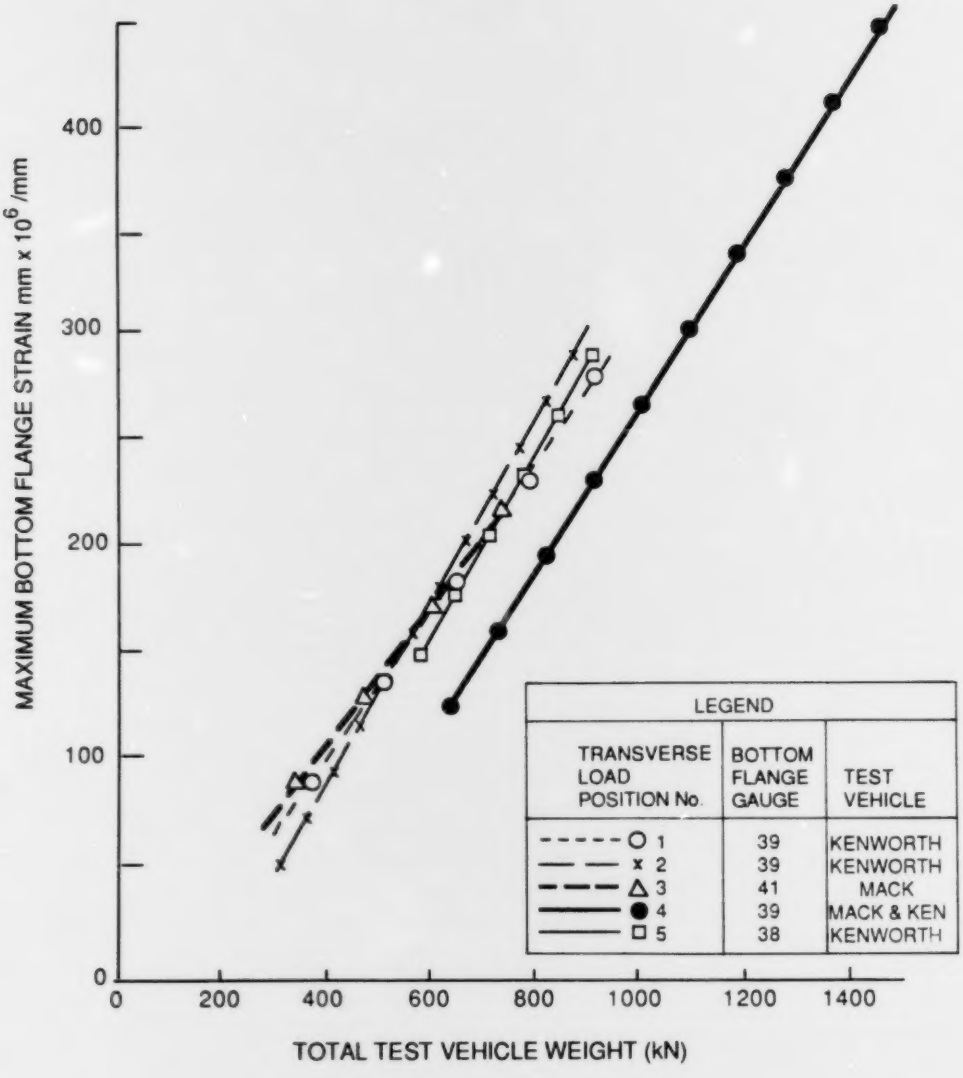

Figure 6.3/ Relationship Between Observed Strain and Load

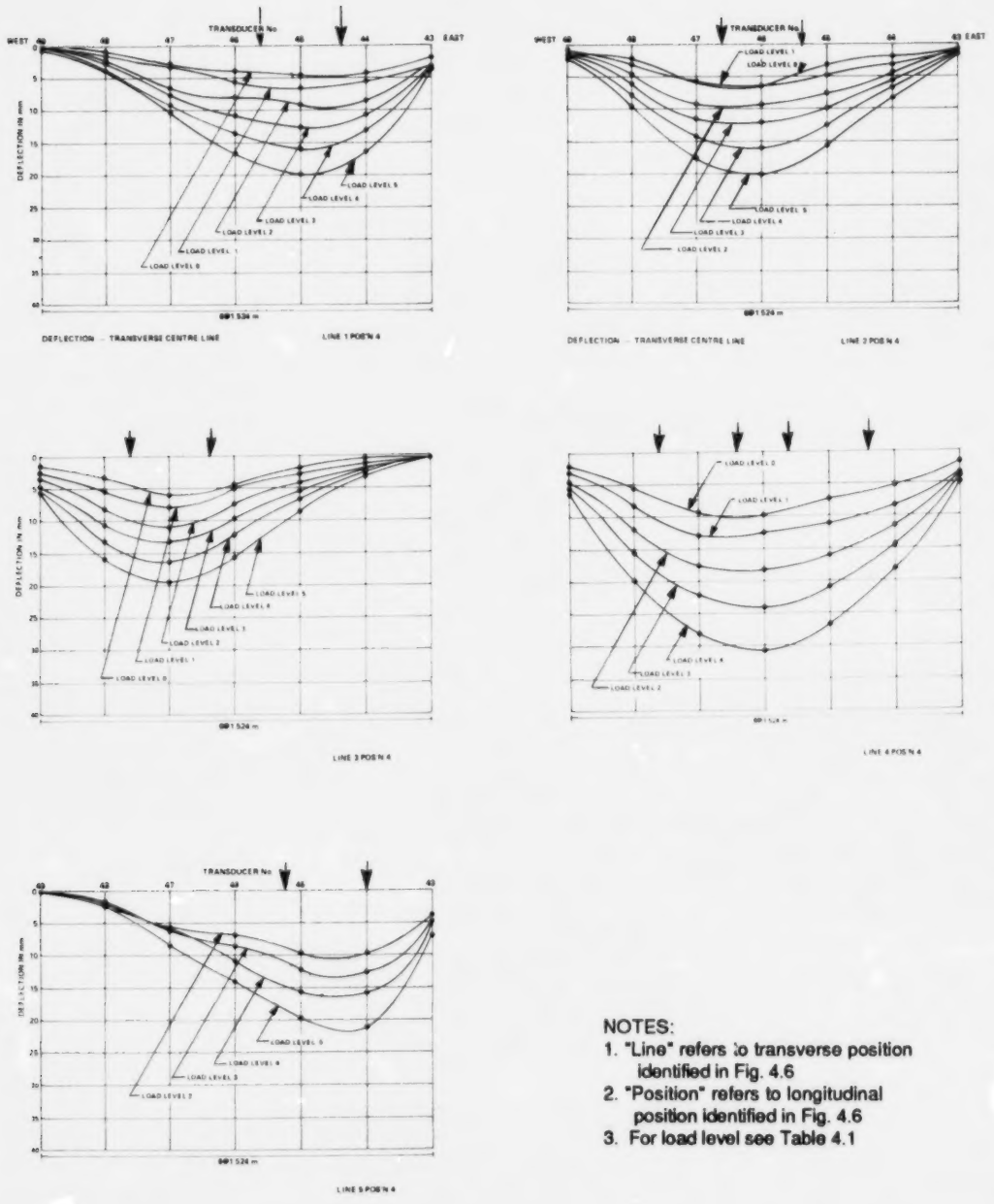

NOTES:
1. "Line" refers to transverse position identified in Fig. 4.6
2. "Position" refers to longitudinal position identified in Fig. 4.6
3. For load level see Table 4.1

Figure 6.4/ Bottom Flange Deflections at Mid-Span

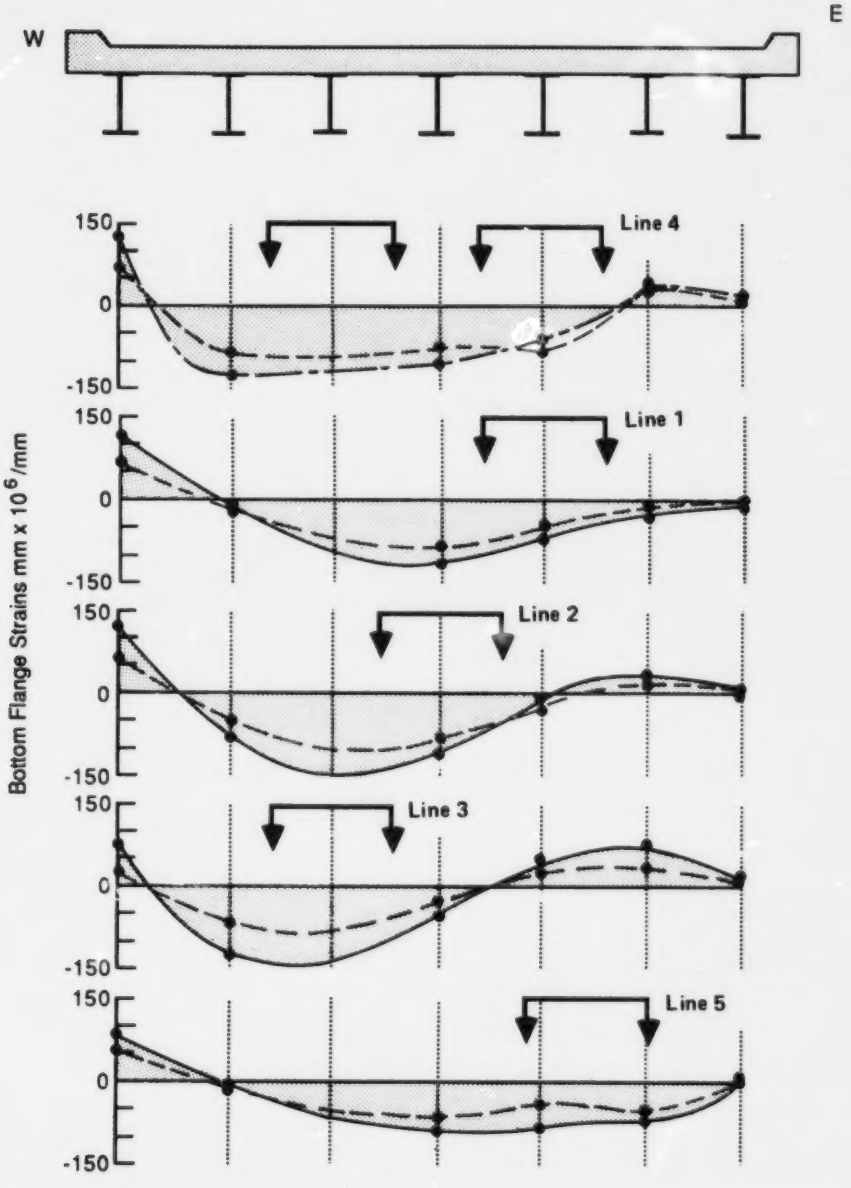

NOTE: Compressive strains shown as-ve

Legend
— — — Load level 2
—·— Load level 4
——— Load level 5

Figure 6.5/ Bottom Flange Strains Near the North Abutment for Longitudinal Load Position No. 4

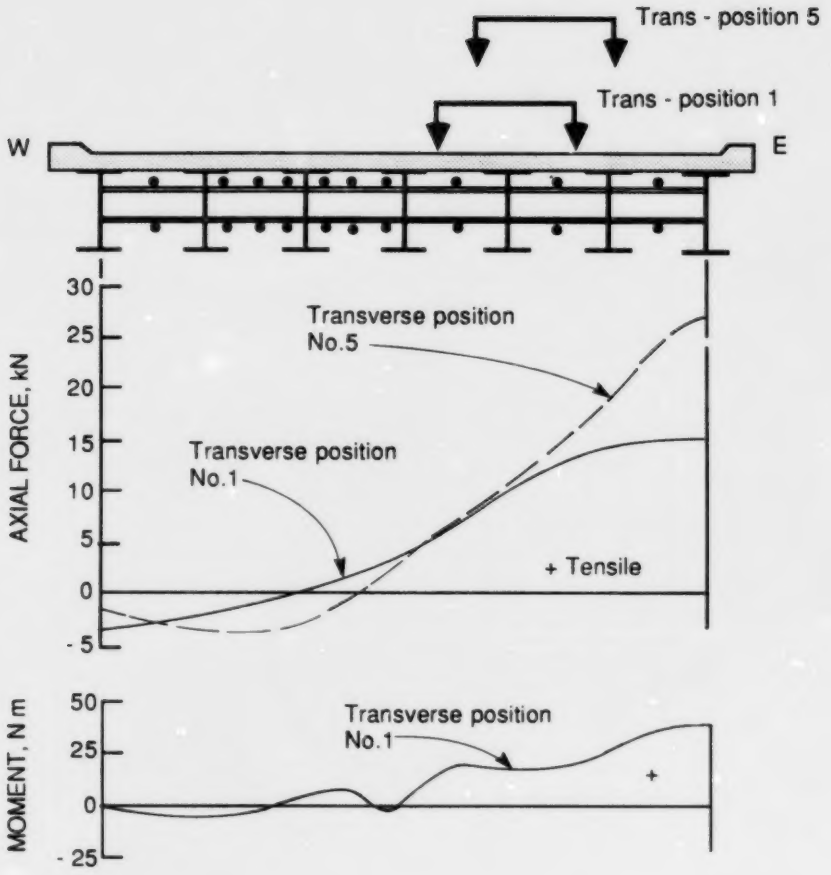

NOTES: (1) Tensile axial force is shown as +ve
(2) Moment causing tension in bottom fibres is shown as +ve

Figure 6.6/ Axial Force and Moment in the North Intermediate Diaphragm Due to Level 5 Load in Longitudinal Position No. 5, and Transverse Position Nos. 1 and 5

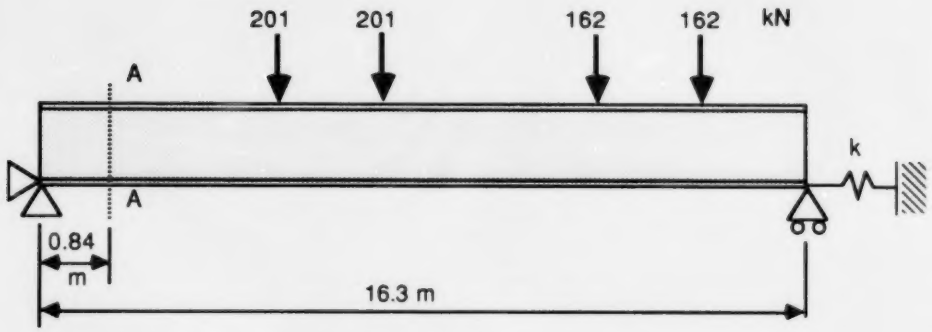

(a) ELEVATION OF GIRDER

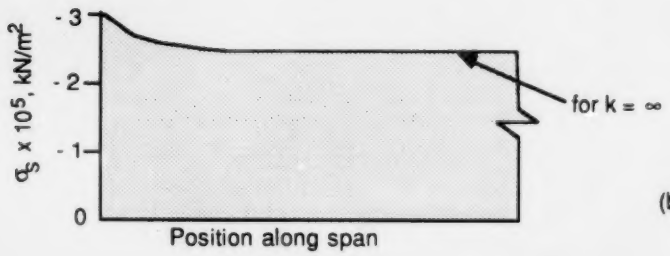

(b) VARIATION OF NET BOTTOM FLANGE STRAINS ALONG SPAN

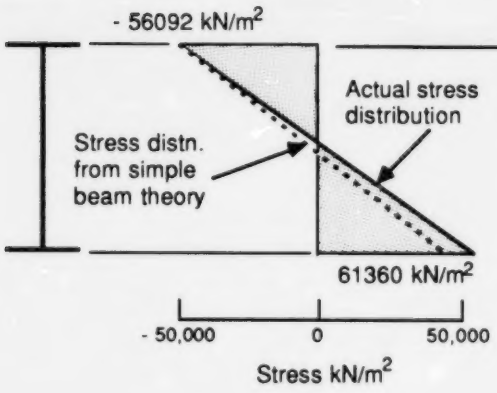

(c) STRESS DISTRIBUTION AT A-A DUE TO BENDING ALONE

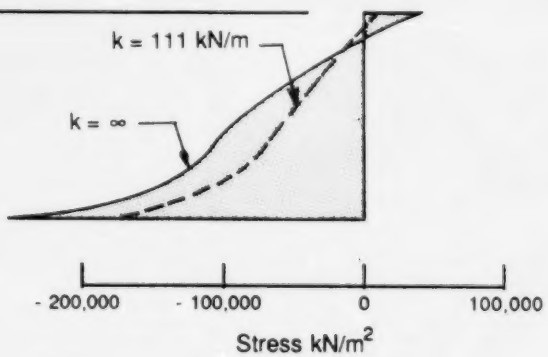

(D) STRESS DISTRIBUTION AT A-A DUE TO BEARING RESTRAINT FORCES ALONE

Figure 7/ Stress Distributed Obtained from 3-D Finite Element Analysis

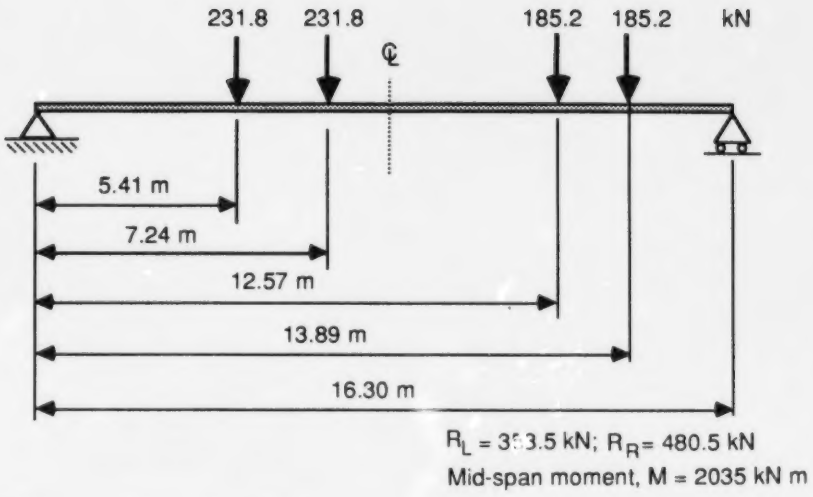

Figure 8.1/ Longitudinal Position of Axles Corresponding to Load Level 5 and Longitudinal Position No. 4

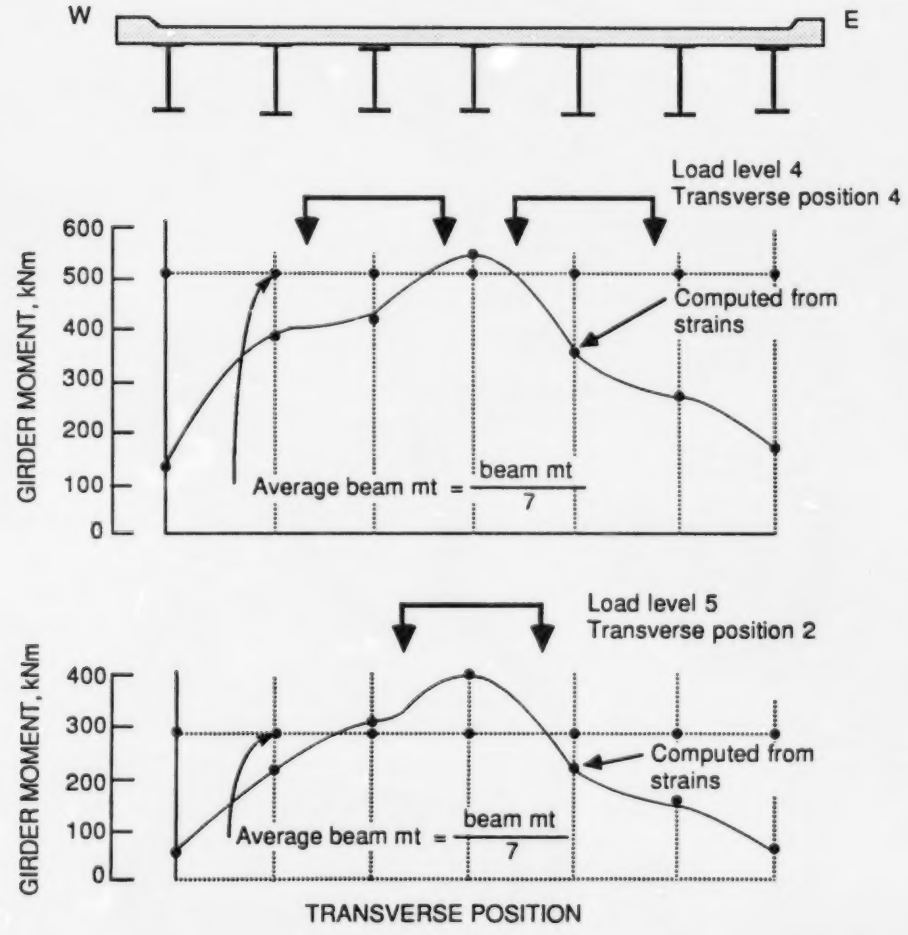

Figure 8.2/ Girder moments Computed from Measured Strains by Ignoring Bearing Restraint Forces

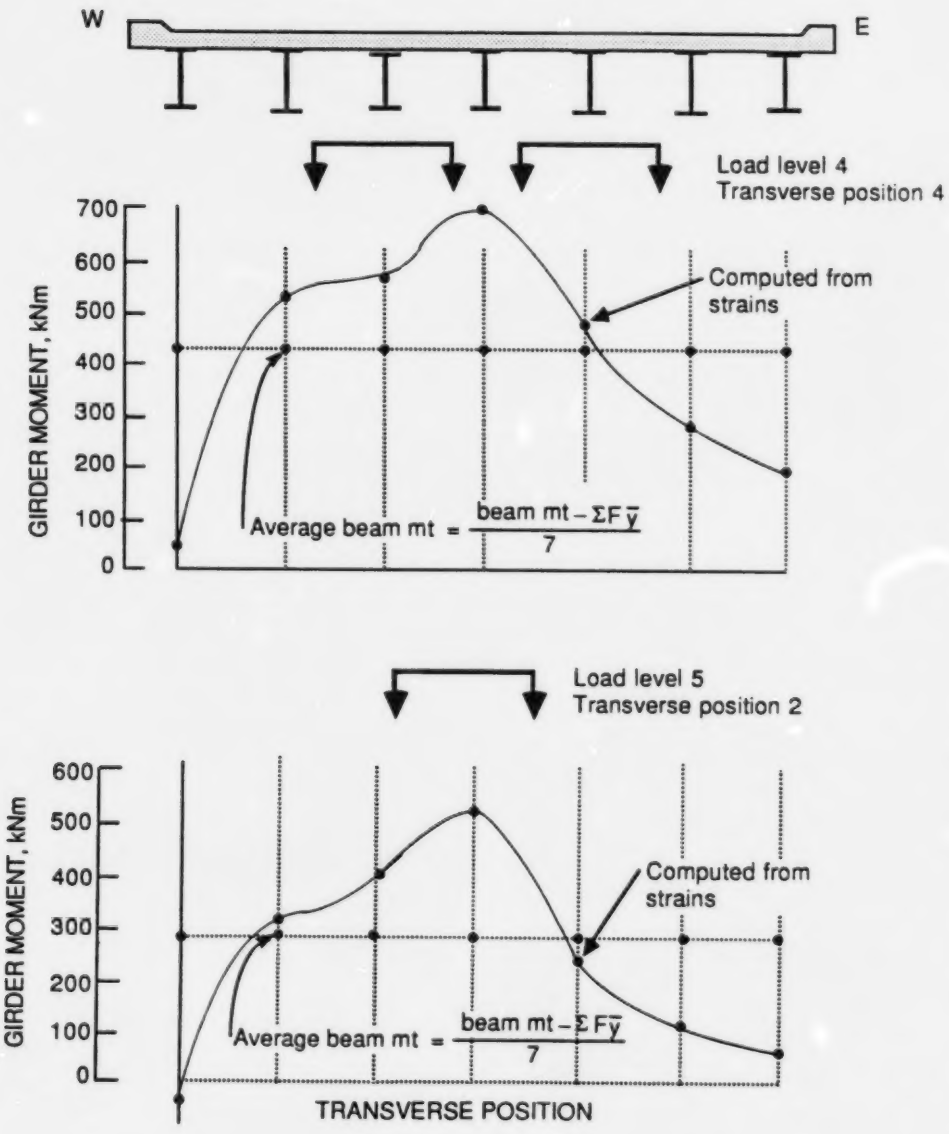

Figure 8.3/ Girder Moments Computed from Measured Strains by Including Bearing Restraint Effects

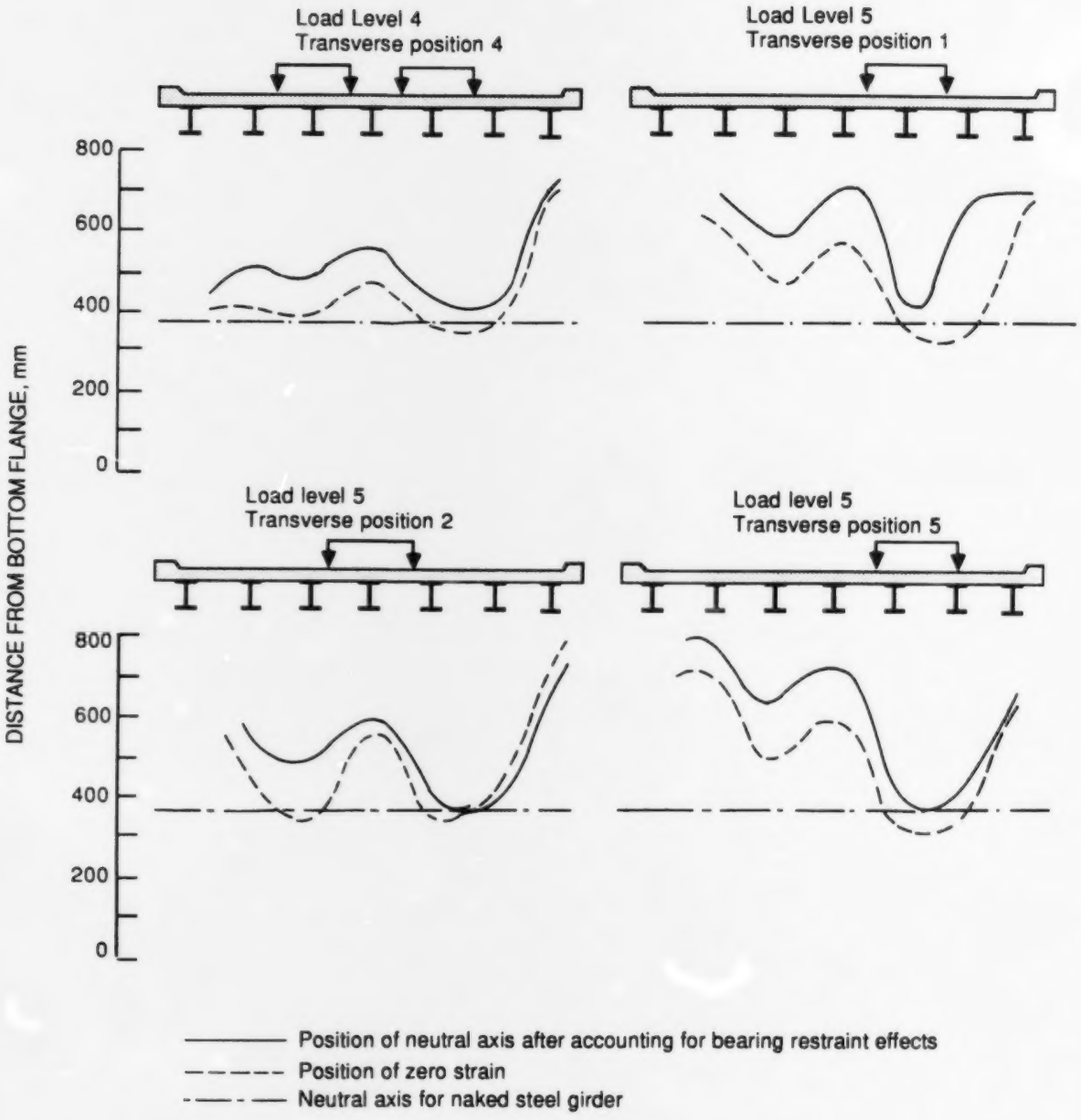

Figure 10.1/ Positions of Neutral Axis at the Mid-Span, as Computed from Measured

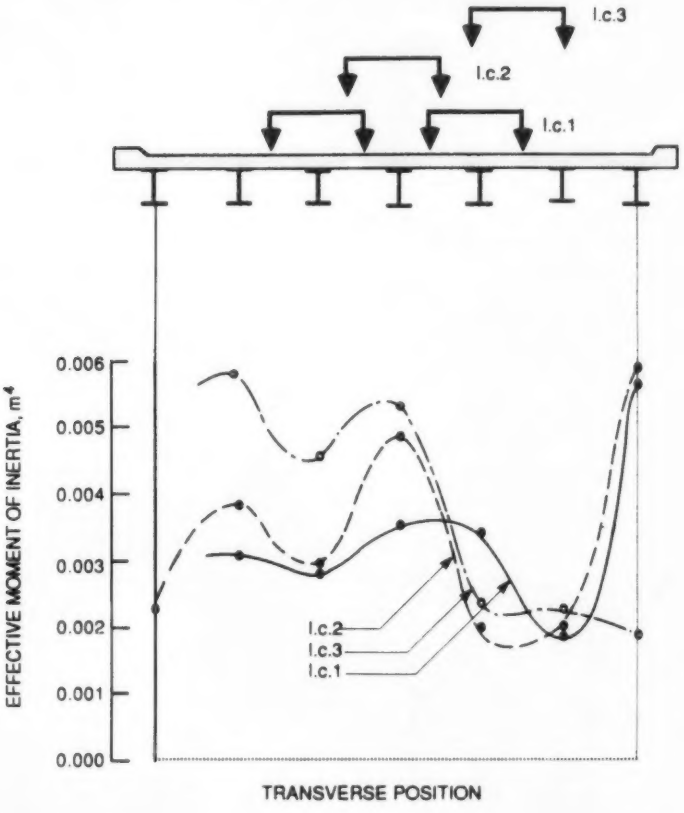

Figure 10.2/ Effective Moments of Inertia of Girders and the Associated Portions of the Deck Slab

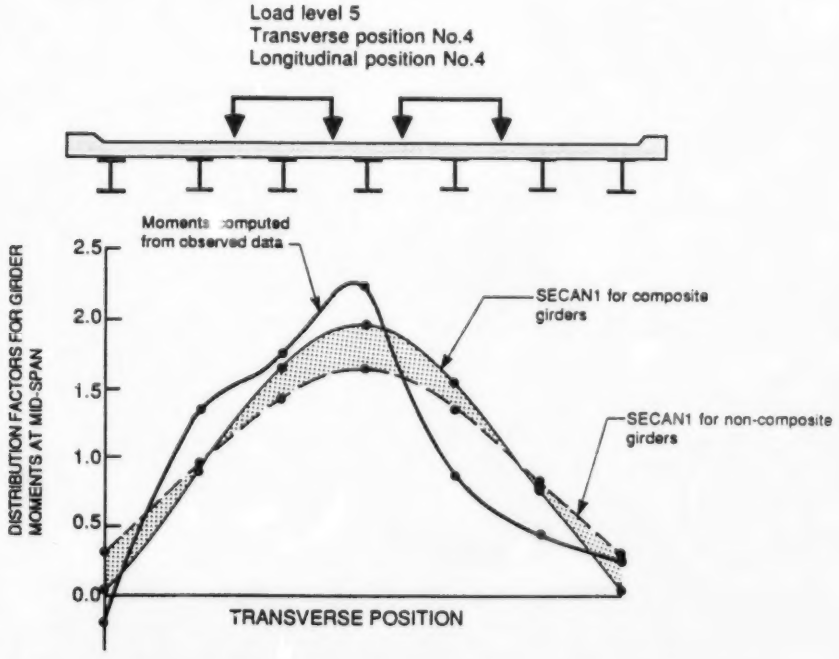

Figure 10.3/ Comparisons of Distribution Factors for Girder Moments at Mid-Span

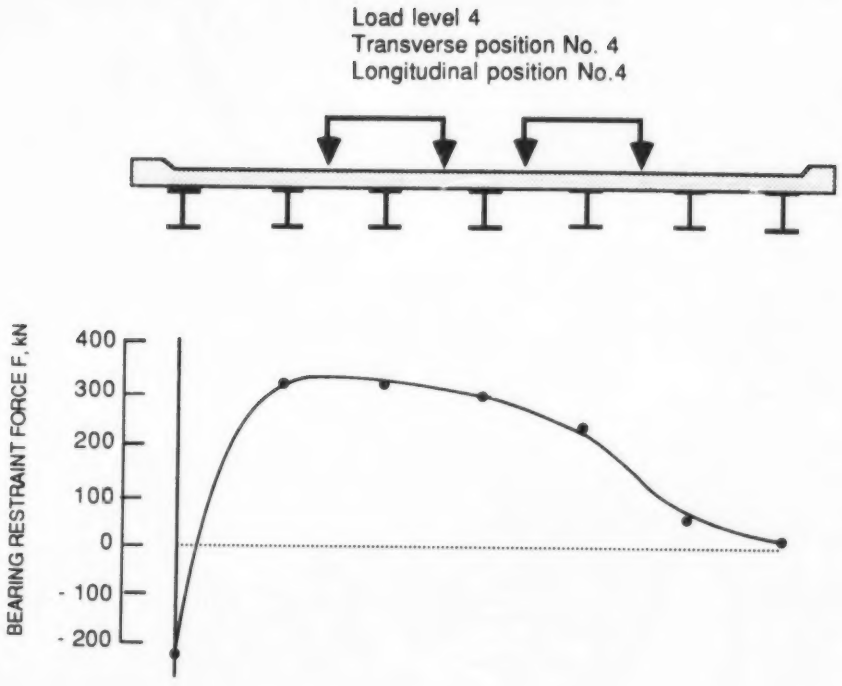

Figure 10.4/ Bearing Restraint for One Particular Load Case

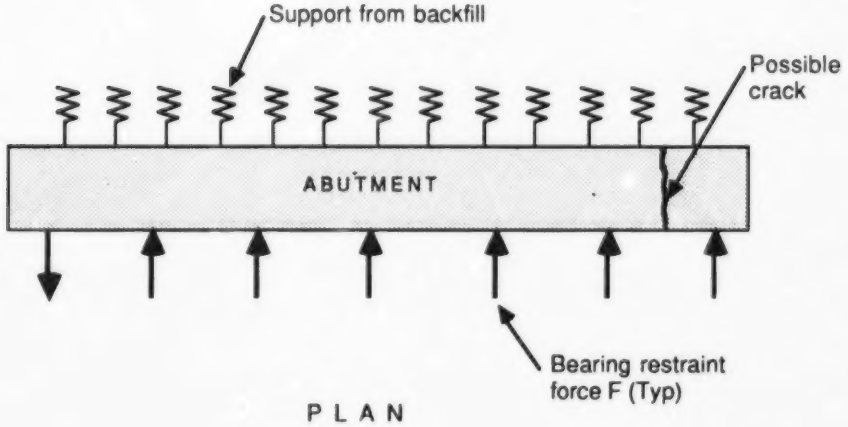

Figure 10.5/ Bearing Restraint Forces for the Case Shown in Fig. 10.4